



King Saud University
Arabian Journal of Chemistry

www.ksu.edu.sa
www.sciencedirect.com



ORIGINAL ARTICLE

Corrosion inhibition, adsorption and thermodynamic properties of poly(vinyl alcohol-cysteine) in molar HCl

Ali Fathima Sabirneeza Abdul Rahiman *, Subhashini Sethumanickam ¹

Department of Chemistry, Avinashilingam Institute for Home Science and Higher Education for Women, Coimbatore, Tamil Nadu 641043, India

Received 26 August 2012; accepted 23 January 2014

KEYWORDS

Mild steel;
Poly(vinyl alcohol-cysteine);
Weight loss;
Polarization;
Impedance spectroscopy;
El-Awady isotherm

Abstract Chemical synthesis of water soluble conducting polymer composite poly(vinyl alcohol-cysteine) [PVAC] was carried out in oxalic acid medium using ammonium persulfate. The composite was characterized by UV, FTIR and SEM–EDX. The corrosion inhibition performance of PVAC on mild steel in molar hydrochloric acid solution was studied by weight loss and electrochemical methods. A maximum inhibition efficiency of 94% was observed in the presence of 0.6 wt% of the inhibitor. The influence of inhibitor concentration, solution temperature, and immersion time on the corrosion of mild steel has been investigated. Polarization measurements showed the mixed type inhibitive nature of the polymer composite. The results obtained from the different methods are in good agreement. The various kinetic and thermodynamic parameters of metal dissolution and composite adsorption processes were evaluated from the weight loss methods in order to elaborate the adsorption mechanism. Adsorption of inhibitor obeyed El-Awady adsorption isotherm.

© 2014 Production and hosting by Elsevier B.V. on behalf of King Saud University.

1. Introduction

Mild steel is an important material of choice due to low cost and easy availability. Acids are deployed in many service

* Corresponding author. Address: Avinashilingam Institute for Home Science and Higher Education for Women, Coimbatore, Tamil Nadu 641043, India. Tel.: +91 9786832898; fax: +91 4912858069.

E-mail addresses: fathima.rahiman@gmail.com (A.F.S. Abdul Rahiman), subash.sethu@gmail.com, subhashini_adu@yahoo.com (S. Sethumanickam).

¹ Tel.: +91 9443381766.

Peer review under responsibility of King Saud University.



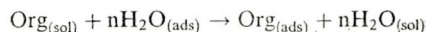
Production and hosting by Elsevier

environments such as pickling, cleaning of boilers, descaling and acidization of oil well. In order to reduce the undesirable base metal dissolution by these processes, corrosion inhibitors are usually added. Research on organic corrosion inhibitors has been mainly focused on the inhibitor structure relationship with its adsorption properties and mechanism. It has been observed that the adsorption acutely depends on specific physico-chemical properties of the inhibitor molecule such as functional groups, steric factors, aromaticity, electron density at the donor atoms, and π -orbital character of donating electrons (Jayalakshmi and Muralidharan, 1998). It also depends on the electronic structure of the molecules (Granese, 1988) and (Granese et al., 1992). Thus the efficiency of an organic compound is mainly dependent on its ability to get adsorbed on the metal surface. Corrosion inhibition is initiated by the displacement of adsorbed water molecules by the inhibitor

1878-5352 © 2014 Production and hosting by Elsevier B.V. on behalf of King Saud University.
<http://dx.doi.org/10.1016/j.arabjc.2014.01.016>

Please cite this article in press as: Abdul Rahiman, A.F.S., Sethumanickam, S. Corrosion inhibition, adsorption and thermodynamic properties of poly(vinyl alcohol-cysteine) in molar HCl. Arabian Journal of Chemistry (2014), <http://dx.doi.org/10.1016/j.arabjc.2014.01.016>

species leading to specific adsorption of the inhibitor onto the metal surface as:



The comparative studies of adsorption behavior and corrosion inhibition ability between monomers and polymers have revealed that polymers are adsorbed stronger than their monomer analogs (Jeyaprabha et al., 2005a and Jeyaprabha et al., 2005b). Different homo-polymers (Umoren et al., 2006 and Aly et al., 2009), copolymers (Yurt et al., 2007 and Srikanth et al., 2006) and conducting polymers (Gelling et al., 2001 and Shukla et al., 2008) have been reported as efficient corrosion inhibitors for metals in acidic media. Umoren, 2009 on his review has given a vivid account of polymeric compounds used as inhibitors for different metals. Hence polymers are better corrosion inhibitors than the corresponding monomers. The improved performances of polymeric materials are attributed to their multiple adsorption sites for bonding with metal surface. The main advantages of polymeric inhibitors are (i) a single polymeric chain displaces many water molecules from the metal surface thus making the process entropically favorable (ii) the presence of multiple bonding sites makes the desorption of polymers a slower process (Amin et al., 2009). Furthermore it has been noticed that both the molecular area (Ayers and Hackerman, 1963) and molecular weight (Yurt et al., 2007) of the inhibitor are of key importance. The polymers with higher molecular weight show higher inhibition efficiency provided the polymers have good solubility (Amin et al., 2009). Amino acids and its derivatives (Yurt et al., 2005 and Taha et al., 1995) were examined for their corrosion inhibition property in acidic environment for different metals. Moreover the biological importance of amino acids shrinks its practical applicability for corrosion inhibition process. The present investigation focused on the synthesis of novel and efficient inhibitor by compositing/doping polyvinyl alcohol (PVA) with L-cysteine. Corrosion inhibition was investigated using potentiodynamic polarization, electrochemical impedance spectroscopy and weight loss method. The doping process increased the efficiency of polyvinyl alcohol from 70% to about 95%.

2. Experimental

2.1. Synthesis of poly(vinyl alcohol-cysteine)

Poly vinyl alcohol ($14,000 \text{ g mol}^{-1}$) and L-cysteine ($121.16 \text{ g mol}^{-1}$) obtained from Merck were used for the synthesis of poly(vinyl alcohol-cysteine) composite. The composite was synthesized according to the procedure described elsewhere (Ali Fathima Sabirneeza et al., 2011 and Ali Fathima Sabirneeza and Subhashini, 2012). 10 g of PVA was dissolved in hot 0.5 M oxalic acid solution, and mixed with 1 g of L-cysteine dissolved in 0.5 M oxalic acid. The mixture was cooled to $0-5^\circ\text{C}$. Freshly prepared ammonium persulfate was added drop wise to the cold mixture with constant stirring. The reaction mixture was stirred well for 2 h using a magnetic stirrer and refrigerated for a day. The system was made slightly alkaline (pH 8-9) with aqueous ammonia and the composite was precipitated by adding a non-solvent (acetone). The composite was filtered under vacuum, washed and air dried. The synthesized composite was characterized by UV, FTIR and SEM-EDX analysis.

6% solution of PVAC in double distilled water is used as a stock solution for corrosion studies. Analar grade hydrochloric acid (Merck) was used to prepare blank 1 M HCl solution.

2.2. Electrochemical measurements

Frequency response analyzer (Solartron model 1280B) controlled with corware and z-plot corrosion software was used for data acquisition and analysis. The conventional three electrode system consisting of saturated calomel electrode (SCE) as reference electrode, platinum foil as counter electrode and mild steel strips having exposed area of 1 cm^2 as working electrode was used. The mild steel specimens used for the studies have the composition (% by weight) 0.196 Mn, 0.106 C, 0.027 P, 0.022 Cr, 0.016 S, 0.012 Ni, 0.006 Si, 0.003 Mo and remainder Fe. The electrodes were immersed in 1 M HCl solution for 30 min until a steady-state potential was reached. All tests were performed at $30 \pm 2^\circ\text{C}$ under static conditions without deaeration. The polarization studies were carried out from a potential of +250 to -250 mV (vs. SCE) with respect to the steady-state potential at a scan rate of 2 mV s^{-1} . Anodic and cathodic Tafel segments were extrapolated to obtain corrosion potential (E_{corr}) and corrosion current density (I_{corr}). The inhibition efficiency was evaluated from the measured I_{corr} values using the relationship.

$$IE_{I_{\text{corr}}}(\%) = \frac{I_{\text{corr}}^0 - I_{\text{corr}}}{I_{\text{corr}}^0} * 100 \quad (1)$$

where, I_{corr}^0 and I_{corr} are the corrosion current density in the absence and presence of inhibitor, respectively.

The corware software directly calculates the linear polarization resistance values on the basis of Stern-Geary theory. Then inhibition efficiency has been calculated from the polarization resistance (R_p) values.

$$IE_{R_p}(\%) = \frac{R_p - R_p^0}{R_p} * 100 \quad (2)$$

where, R_p^0 and R_p are the polarization resistance in the absence and presence of the inhibitor, respectively.

Electrochemical Impedance measurements were carried out using AC signals of 10 mV amplitude and sweeping the frequency from 20 kHz to 0.1 Hz. The electrode (MS) was immersed for 30 min in 1 M HCl before starting measurement to attain the steady state. The impedance data were analyzed with Zsimpwin software. The charge transfer resistance obtained by fitting the semicircles of the Nyquist representations has been used to calculate inhibition efficiencies of PVAC,

$$IE_{R_{\text{ct}}}(\%) = \frac{R_{\text{ct}} - R_{\text{ct}}^0}{R_{\text{ct}}} * 100 \quad (3)$$

where, R_{ct}^0 and R_{ct} are the charge transfer resistance in the absence and presence of the inhibitor, respectively. The double layer capacitance was obtained from the maximum value of the imaginary component of the Nyquist plots.

2.3. Weight loss measurements

Weight loss measurements were performed with the dried rectangular strips ($1 \times 5 \times 0.15 \text{ cm}$) following the ASTM standard procedure (ASTM G 1-2, 1996). The strips were immersed in triplicates in 1 M HCl in the absence and presence of various

concentrations of PVAC for different immersion periods at room temperature. At elevated temperatures, a constant immersion period of 1/2 h was selected and studies were conducted for various concentrations of PVAC. The strips were taken out, cleaned and reweighed. From the obtained weight loss, inhibition efficiency and surface coverage values were calculated using the following equations.

$$IE_W(\%) = \frac{W^0 - W}{W^0} * 100 \quad (4)$$

$$\theta = \frac{W^0 - W}{W^0} \quad (5)$$

where, W^0 and W are the weight losses in g in the absence and presence of inhibitor, respectively.

3. Results and discussion

3.1. Characterization of polymer composites

The synthesized inhibitor PVAC was characterized using UV-Visible Spectroscopy (Systronics double beam spectrophotometer-2202) and FTIR spectroscopy (Bruker-Tensor 27 spectrometer). The surface morphology of the composite was recorded using FEI quanta 200 analyzer.

The UV-Visible spectra of water soluble PVAC gave absorption bands at 234 and 482 nm which are due to $n-\pi^*$ and $\pi-\pi^*$ transitions of the composite respectively. Fig. 1 shows the FTIR spectra of PVA and the composite (PVAC). PVA showed peaks for OH ($3500-3200\text{ cm}^{-1}$), CH ($3000-2800\text{ cm}^{-1}$), C-O and C-C ($1960-1750\text{ cm}^{-1}$) stretching and bending vibrations. The composite showed a broad band at $3498-2735\text{ cm}^{-1}$. This is attributed to the overlapping of NH stretching of polycysteine and OH group of polyvinyl alcohol. C-N stretching band was observed at 2165 cm^{-1} . The band at 1638 cm^{-1} clearly indicates the presence of amide carbonyl group. The deformation bands are observed near $800-500\text{ cm}^{-1}$. The absence of the bands in the region $1730-1700\text{ cm}^{-1}$ confirms the absence of free carboxylic acid group.

The scanning electron micrograph shown in Fig. 2 depicts the surface morphology of the synthesized polymer composite PVAC. This SEM image clearly shows the presence of small ratio of secondary phase - polymerized cysteine which was

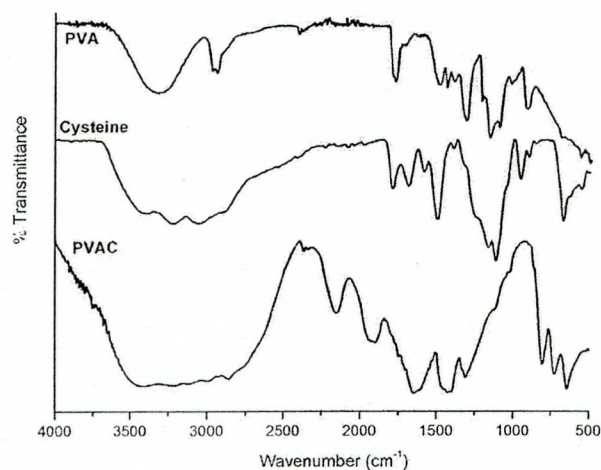


Figure 1 FTIR spectrum of PVA and PVAC.

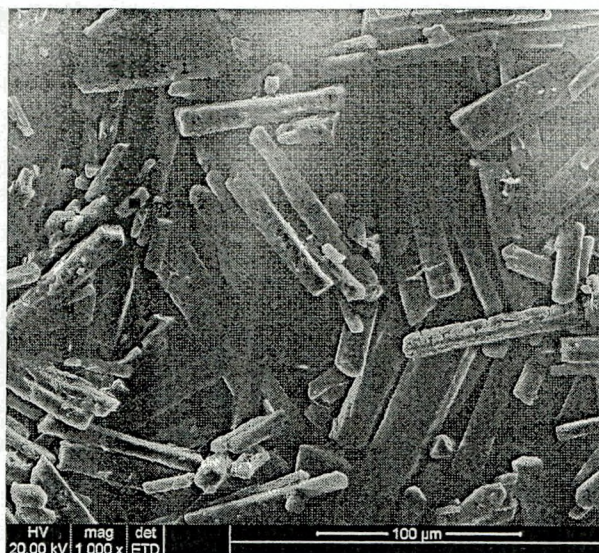


Figure 2 Scanning electron micrograph of PVAC.

randomly distributed and adhered on the polyvinyl alcohol matrix. The weight percent of the elements of the two phases obtained from the EDX analysis is represented in Table 1. Spot 2 counts for about 19 wt% nitrogen and 13 wt% sulfur whereas spot 1 contains only negligible amounts. This confirms the formation of the composite material and hydrogen bonding is the force that holds the polycysteine to PVA matrix.

The AC conductance of the composite was measured by the LCZ analyzer by varying the frequency from 3 MHz to 300 Hz. The composite was made into a pellet of diameter 11.01 mm having a thickness of 2.91 mm. The electrical connection was made using silver paste and copper wires. It was found that the conductance of the composite is in the range of $10^{-6}-10^{-4}\text{ Scm}^{-1}$, which lies in the range of semiconductors ($10^3-10^8\text{ Scm}^{-1}$). Fig. 3 shows the variation of conductance of the composite with operating frequency. The composite differs from the well known conducting polymers such as polyaniline and polypyrrole. The polyaniline and polypyrrole are conducting because of the extended aromatic chains through which electron transfer occurs whereas in the case of PVAC such structures are not available. The conductance of PVAC may be due to the ionic conductivity as it consists of large number of electronegative atoms like nitrogen, oxygen and sulfur throughout the chain.

3.2. Electrochemical measurements

3.2.1. Potentiodynamic polarization studies

Fig. 4 shows the potentiodynamic polarization curves for mild steel in 1 M HCl in the absence and presence of various con-

Table 1 EDX Analysis of PVAC.

Element	Spot-1		Spot-2	
	Wt%	At%	Wt%	At%
C	79.54	83.92	42.79	51.67
N	00.63	00.51	18.58	19.30
O	19.56	15.44	25.21	22.93
S	00.27	00.13	13.42	06.10

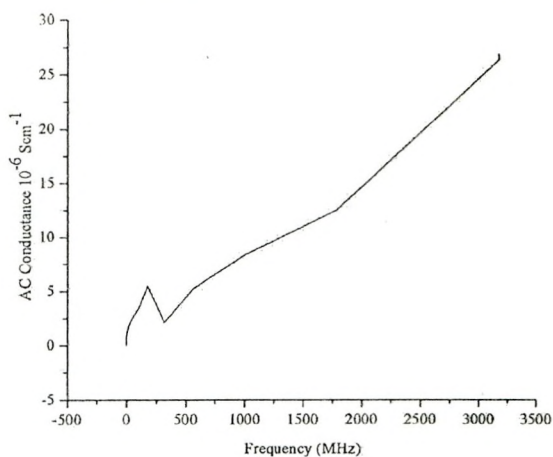


Figure 3 Variation of AC conductance of PVAC with operating frequency.

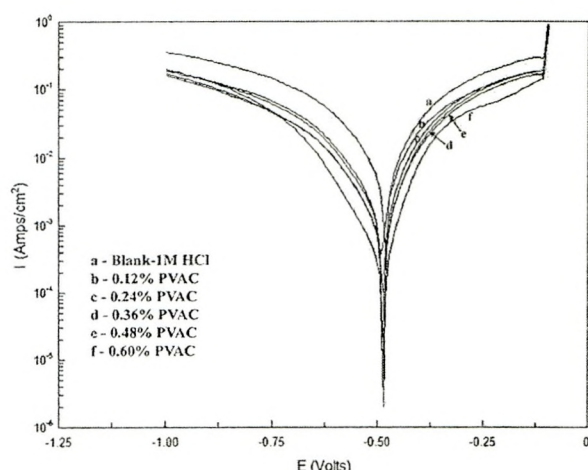


Figure 4 Potentiodynamic polarization curves for mild steel corrosion in the presence of PVAC.

concentrations of PVAC. Table 2 represents the electrochemical parameters such as corrosion potential (E_{corr}), corrosion current density (I_{corr}), Tafel slopes (b_c and b_a) and inhibition efficiencies (IE) for MS acid corrosion in the presence of different concentrations of PVAC. The cathodic and anodic Tafel slopes of the curves were shifted toward the low potential region as the inhibitor concentration increases. This indicates that the inhibitor controlled both the cathodic and anodic reactions

and thus behaved as a mixed type inhibitor (Abdel-Rehim et al., 2006). It is also observed that the E_{corr} values did not change significantly in the presence of the composites suggesting that the inhibitors are mixed type inhibitors. At more positive potential region hydrogen evolution is the competing process whereas adsorption favors at the less positive potential region. It is evident that the presence of inhibitor even at low concentrations reduces the current density value at constant potential and the suppression in current density increases ($9.05\text{--}0.65\text{ mA/cm}^2$) as the concentration of the PVAC increases.

Linear polarization resistance was obtained for the potential range -0.02 to $+0.02$ mV with respect to the open circuit potential. The polarization resistance and the inhibition efficiencies are presented in Table 2. It is clearly observed that in the presence of PVAC the resistance increases considerably which results in an increase in inhibition efficiency (See Table 2).

3.2.2. AC impedance studies

Impedance spectroscopy was used as an additional electrochemical tool, to study the response of mild steel specimen in the presence PVAC toward acidic solution. This technique is useful in the determination of the double layer capacitance and charge transfer resistance of the system. In order to study the adsorption behavior of the composite on MS surface, the impedance responses were taken and its Nyquist representations are shown in Fig. 5. It is clear from the representations that the plots are not perfect semicircles and this may be due to the frequency dispersion. The experimental values of R_{ct} and C_{dl} are presented in Table 3. It could be seen from the table that as the PVAC concentration increases, the R_{ct} values increase and the C_{dl} values tend to decrease. This is attributed to the increase in the surface coverage by the inhibitors leading to an increase in inhibition efficiency. A decrease in the local dielectric constant and/or an increase in the thickness of the electrical double layer are responsible for the decrease in C_{dl} values. The changes in R_{ct} and C_{dl} values were caused by the gradual replacement of water molecules by the composites on the metal surface. This decreases the extent of metal dissolution (Quraishi and Sardar, 2003).

3.3. Weight loss method

3.3.1. Weight loss, corrosion rate and inhibition efficiency

The anodic dissolution of iron in acidic media and the corresponding cathodic reaction have been reported to proceed as follows (Yurt et al., 2004),

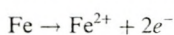
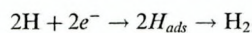


Table 2 Polarization parameters for mild steel acid corrosion in the absence and presence of various concentrations of PVAC.

Conc. of PVAC (% in g)	Tafel extrapolation method (TEM)				LPR method		
	b_a mV/dec	b_c mV/dec	E_{corr} mVvs.SCE	I_{corr} mA/cm ²	IE%	R_p Ω	IE%
Blank	181.84	141.14	-481.09	9.05	—	3.83	—
0.12	127.60	89.85	-485.26	2.94	67.15	8.85	56.72
0.24	95.60	70.25	-477.77	2.29	74.70	11.38	66.34
0.36	133.49	90.79	-484.84	1.48	83.65	17.51	78.13
0.48	143.53	75.18	-473.24	1.12	87.62	25.16	84.78
0.60	95.72	85.39	-477.59	0.65	92.82	40.06	90.04

Table 3 Electrochemical impedance parameters for mild steel in 1 M HCl in the absence and presence of various concentrations of PVAC.

Conc of PVAC% in g	Double layer capacitance, C_{dl} mF	Surface coverage θ	Charge transfer resistance R_{ct} Ω	Inhibition efficiency%
Blank	0.452	—	9.37	—
0.12	0.221	0.5110	30.29	69.06
0.24	0.174	0.6150	44.26	78.83
0.36	0.131	0.7102	61.54	84.77
0.48	0.085	0.8119	132.37	92.64
0.60	0.109	0.7588	203.34	95.39



As a result of these reactions, including the high solubility of the corrosion products, the metal loses its weight in the solution. The corrosion inhibition performance of PVAC against uniform corrosion was investigated by monitoring the weight loss occurred during the process. The inhibition efficiencies were calculated from the weight loss and its variation with immersion time for different concentrations of PVAC is shown in Fig. 6. The figure also includes the inhibition efficiency obtained for 0.6 wt% of PVA which was only 72.5%. On compositing 0.0045 mol of cysteine with polyvinyl alcohol, the inhibition efficiency increases to 94.2%. It is also apparent that the inhibition efficiency has increased from 78% to 94% as the concentration of PVAC increased from 0.06 to 0.6 wt%. The maximum inhibition efficiency was observed at 0.6% PVAC and any further increase in concentration did not cause any appreciable change in the performance of the inhibitor thereby indicating the attainment of the limiting value. This effect may be due to the accumulation of the composites onto the positively charged metal surface, which reduces the direct contact of the metal and the corrosive environment. The electrostatic interactions between the metal surface and the composite made the accumulated PVAC to get adsorbed on the surface. The higher performance of the composite is attributed to the presence of nitrogen and oxygen atoms, larger molecular size and linearity in the polymeric chain. As the immersion time increases, the inhibition performance also increases. The maximum IE value was obtained for 6 h immersion then a slight decrease in IE was observed. As the time passes on the stability

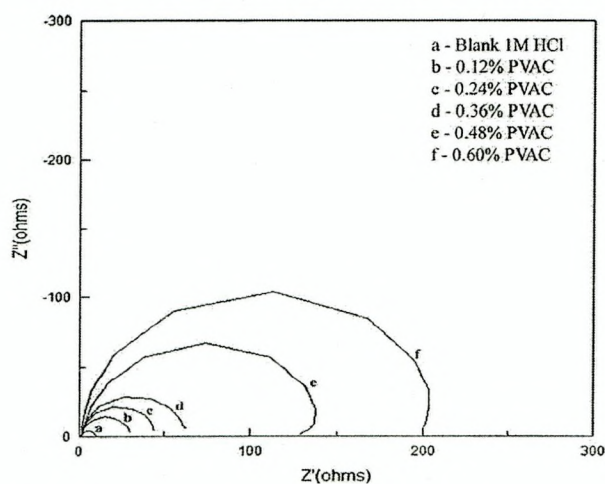


Figure 5 Nyquist representations for mild steel corrosion in the presence of PVAC.

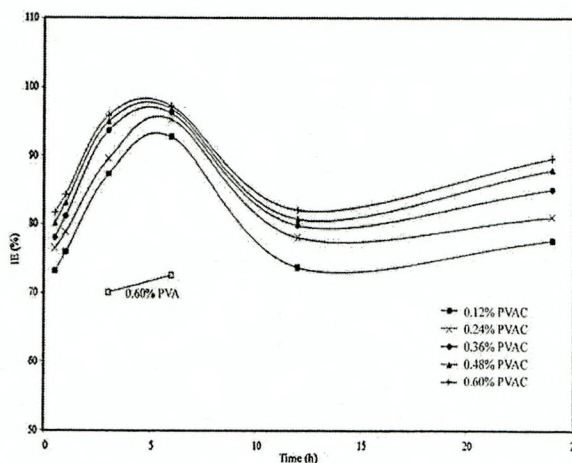


Figure 6 Variation of inhibition efficiency of PVAC with immersion time at 30 °C.

of adsorbed film decreases and results in desorption to attain the equilibrium.

3.3.2. Effect of temperature

The temperature can modify the interactions between the mild steel and the acidic medium in the absence and presence of the inhibitors. Results obtained from the weight loss measurements for mild steel in 1 M HCl in the temperature range 30–70 °C are shown in Fig. 7. The inhibition efficiency increases with temperature up to 50 °C, which indicates the stability of the adsorbed film at the studied temperatures. The increase in IE may be due to the formation of free (non hydrogen bonded) OH and NH groups and/or the physically adsorbed composite may be involved in chemical interaction with the mild steel. With further increase in temperature the inhibition efficiency decreases. This is due to the instability of the adsorbed film above 50 °C. The increase in temperature shifts the equilibrium in favor of desorption process than the adsorption process (Wahyuningrum et al., 2008).

3.3.3. Activation parameters of corrosion process

The corrosion rates evaluated at different temperatures in the absence and presence of PVAC were used to calculate the activation energy of the metal dissolution. Most of authors used Arrhenius equation to calculate the apparent activation energy of corrosion process (Quraishi and Khan, 2005, Breslin and Carrol, 1993 and Khedr and Lashien, 1992) of mild steel in acid medium,

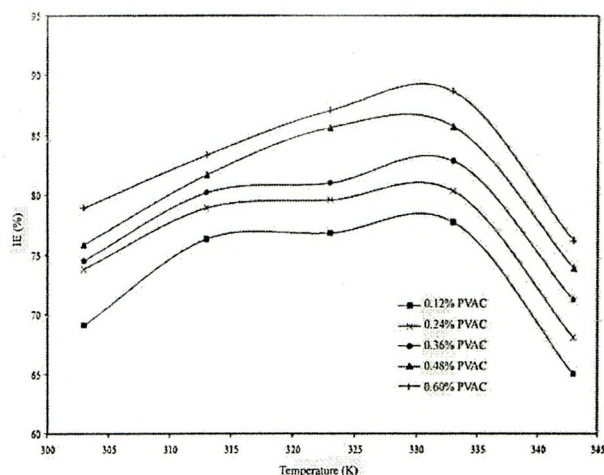


Figure 7 Variation of inhibition efficiency of PVAC with immersion temperature for $\frac{1}{2}$ h immersion in stagnant solution.

$$\log CR = \frac{-E_a}{2.303RT} + \log \lambda \quad (6)$$

where, CR is the corrosion rate, E_a is the activation energy, λ is the Arrhenius pre exponential factor, R is the gas constant expressed in $\text{JK}^{-1}\text{mol}^{-1}$ and T is the absolute temperature. The E_a and λ values obtained from the slope and intercept of the Arrhenius plots (Fig. 8) are given in Table 4. The data showed that the activation energy for the corrosion of mild steel in 1 M HCl in the presence of inhibitor is higher than that of free acid. This indicated that the used inhibitors considerably increase the activation energy of the corrosion process due to their adsorption onto the metal surface (Negm and Zaki, 2008 and Negm et al., 2009). In the literature, the lower activation energy value for corrosion process in the presence of the inhibitor is attributed to its chemisorption, while the higher value is associated with its physical adsorption (Labrabi et al., 2005). The increased activation energy in the presence of the inhibitor suggests that adsorbed polymer composites create a physical barrier to charge and mass transfer, leading to reduction in corrosion rate (Oguzie, 2006). The value of λ is also higher

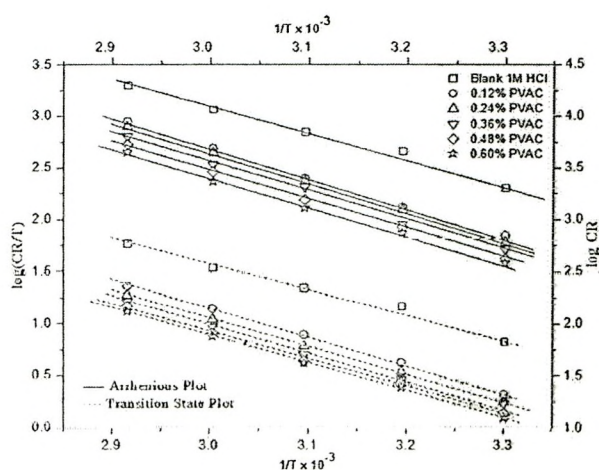


Figure 8 Arrhenius and Transition plots for mild steel corrosion in the presence of PVAC.

for the inhibited solutions than the uninhibited one. The Arrhenius equation suggests the influence of E_a and λ on the corrosion rate. The variation of both E_a and λ with concentration reveals that activation energy is the deciding factor rather than λ .

The values of enthalpy of activation (ΔH_o) and entropy of activation (ΔS_o) were calculated using the following equation (Bentiss et al., 2005).

$$CR = \frac{RT}{Nh} \exp\left(\frac{\Delta S_o}{R}\right) \exp\left(-\frac{\Delta H_o}{RT}\right) \quad (7)$$

where, h is the Planck's constant and N is the Avogadro's number. A plot of $\log(CR/T)$ versus $1/T$, (Fig. 8-transition state plot) gave a straight line with slope $(-\Delta H_o/2.303R)$ and intercept of $[\log(R/Nh) + (\Delta S_o/2.303R)]$ from which ΔH_o and ΔS_o were calculated and listed in Table 4. The positive values of ΔH_o in the absence and presence of inhibitor reflect the endothermic nature of metal dissolution process, which suggested the slow dissolution of mild steel (Benali et al., 2005). It is evident from the table that the value of ΔH_o increased in the presence of PVAC than the uninhibited solution indicating higher protection efficiency. Comparing the values of ΔS_o it is clear that the entropy of activation decreased in the presence of the studied inhibitor than that of the free acid. The low value of ΔS_o supports the slower metal dissolution in the presence of PVAC.

The change in free energy of activation ΔG_o for the corrosion process can be calculated at each temperature applying the thermodynamic relation,

$$\Delta G_o = \Delta H_o - T\Delta S_o \quad (8)$$

The obtained values of ΔG_o are listed in Table 4. The values were positive and increased with an increase in temperature. With an increase in temperature the spontaneity of the corrosion process increases indicating the solubility of the activated complex at higher temperatures. With the increase in concentration the free energy of activation increases, and ascribed to the formation of unstable activated complex in the rate determining transition state.

3.3.4. Adsorption isotherm and adsorption parameters

Basic information on the interaction between the inhibitor and the mild steel surface can be provided by the adsorption isotherm. In order to obtain the isotherm, the linear relation between θ values and C_{inh} must be found. Attempts were made to fit the θ values to various isotherms including Langmuir, Temkin, Frumkin and Flory-Huggins. By far the best fit is obtained with the Langmuir isotherm. This model has also been used for other inhibitor systems (Lagrecee et al., 2002 and Bentiss et al., 2002). According to this isotherm, θ is related to C_{inh} by the relation,

$$K.C_{inh} = \frac{\theta}{1-\theta} \quad (9)$$

where, K is the equilibrium constant of the adsorption-desorption process.

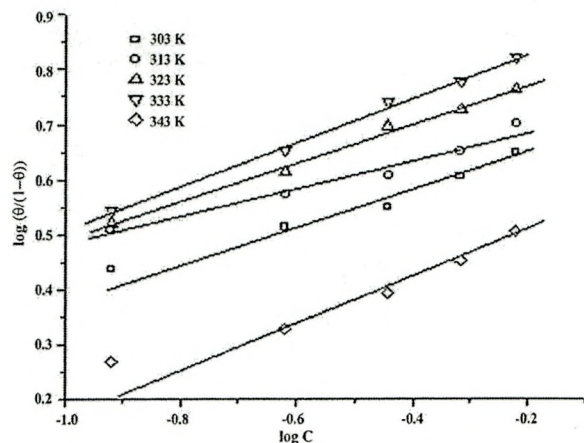
The expected relationship was obtained for all the studied temperatures but the slopes are largely deviated from the unity. By testing the other isotherms, it is found that the experimental data fit the El-Awady adsorption isotherm. The El-Awady adsorption isotherm is formulated as,

Table 4 Activation parameters of mild steel corrosion in the presence of PVAC in 1 M HCl.

Conc of PVAC (%)	E_a kJ/mol	$\lambda \cdot 10^{11}$	ΔH_o J/mol	ΔS_o J/Kmol	$+\Delta G_o$ (kJ/mol)				
					30 °C	40 °C	50 °C	60 °C	70 °C
Blank	43.76	1.58	45.06	-40.68	12.37	12.78	13.19	13.59	14.00
0.12	52.46	6.86	49.78	-53.75	16.34	16.87	17.41	17.95	18.49
0.24	51.45	8.38	48.77	-58.59	17.80	18.39	18.97	19.56	20.14
0.36	49.46	15.9	46.78	-65.92	20.02	20.68	21.33	22.00	22.66
0.48	48.10	87.1	45.22	-71.48	21.70	22.42	23.13	23.85	24.56
0.60	48.42	85.4	45.09	-73.00	22.16	22.89	23.62	24.35	25.08

$$\log \left(\frac{\theta}{1-\theta} \right) = \log K' + y \log C_{inh} \quad (10)$$

where, K' is the equilibrium constant for the adsorption process; and is related to K as $K = K'^{1/y}$, y represents the number of water molecules replaced by one inhibitor molecule. The value of $1/y$ less than unity implies the multilayer adsorption whereas the value greater than unity indicates the given inhibitor occupies more than one active site (Obot et al., 2009, shukla and Ebenso, 2011 and Singh and Quraishi, 2011). The curve fitting of the El-Awady model is shown in Fig. 9 and the calculated values of K , K' , $1/y$ and correlation coefficient are listed in Table 5. The strong correlations confirm the validity of the approach. The higher values of y confirm that the single polymer molecule replaces three to four water molecules from the mild steel surface. Alternatively lower $1/y$ values suggested the multilayer physisorption of PVAC molecules.

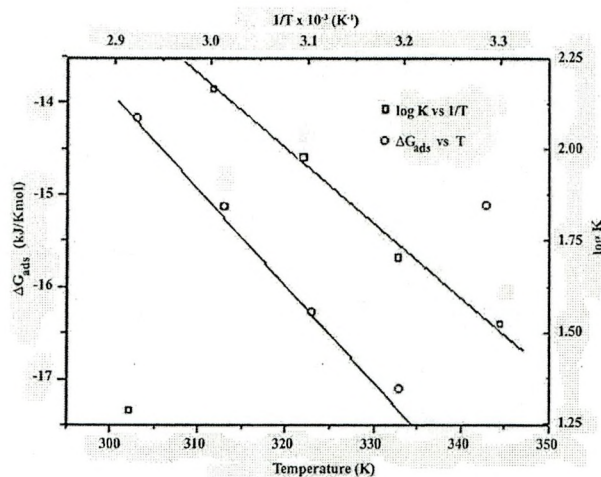
**Figure 9** El-Awady isotherm for PVAC adsorption on mild steel.

The value of K is related to the standard free energy of adsorption, ΔG_{ads} by the following equation (Bentiss et al., 2005),

$$K = \frac{1}{55.5} \exp \left(\frac{-\Delta G_{ads}}{RT} \right) \quad (11)$$

The value 55.5 is the concentration of water in solution. The values of ΔG_{ads} on mild steel at various temperatures are calculated and presented in Table 5. The negative values of ΔG_{ads} suggest that the adsorption of the composites is a spontaneous process (Ebenso and Obot, 2010). And also the values are less than -40 kJ/mol. These lower values are attributed to the electrostatic interaction between the composites and the metal surface (physisorption).

The other important thermodynamic parameters are the enthalpy and entropy of adsorption, which are calculated from van't Hoff equation,

**Figure 10** Plots of $\ln K$ against $1/T$ and ΔG_{ads} vs. T for PVAC adsorption on mild steel.**Table 5** Adsorption parameters of mild steel corrosion in the presence of PVAC in 1 M HCl.

Temp K	K	K'	y	R^2	$-\Delta G_{ads}$ (kJ/mol)	$-\Delta H_{ads}$ kJ/mol	ΔS_{ads} J/Kmol
303	5.00	236.93	3.39	0.9876	14.17		
313	5.48	705.50	3.85	0.9827	14.88		
323	7.73	110.00	2.30	0.9373	16.28	1.08*	44.68*
333	8.69	99.58	2.13	0.9450	17.11	2.23#	41.12#
343	3.61	47.18	3.00	0.9781	15.12		

* Parameters calculated from van't Hoff equation.

Parameters calculated from basic thermodynamic equation.

$$\ln K = -\frac{\Delta H_{ads}}{RT} + \frac{\Delta S_{ads}}{R} + \ln \frac{1}{55.5} \quad (12)$$

and the basic thermodynamic equation (Musa et al., 2009) are presented in Table 5. In order to calculate enthalpy and entropy of adsorption $\ln K$ was plotted against $1/T$ (Fig. 10). From the slope ($-\Delta H_{ads}/R$) and intercept ($\Delta S_{ads}/R + \ln 1/55.5$) ΔH_{ads} and ΔS_{ads} are calculated and presented in Table 5. The low negative values of enthalpy and the large positive values of entropy of adsorption indicate the spontaneity of the process. This is attributed to the endothermic nature of the adsorption process accompanied by the increase in entropy (Negm and Zaki, 2008). The plot of ΔG_{ads} against T was also used to calculate enthalpy and entropy of adsorption (Fig. 10). The slope of straight line gives $-\Delta S_{ads}$ and the intercept, enthalpy of adsorption (Table 5). These results corroborated a strong adsorption of the composites on the metal surface (Gomma and Wahdan, 1995). The enthalpy and

entropy of adsorption obtained from both methods are in good agreement.

3.4. Scanning electron microscope

To establish whether inhibition is due to the formation of a film on the metal surface via adsorption scanning electron photographs were taken. Fig. 11 shows the mild steel surface before immersion and after immersion in acid (6 h) whereas Fig. 12 is of mild steel immersed in 1 M HCl containing PVAC after 6 h. It was found that an adsorbed layer is formed on mild steel, which inhibits corrosion. The protection provided by PVAC to mild steel in 1 M HCl solutions was retained, when specimen dipped in acid without inhibitor. This observation clearly proves that the inhibition is due to the formation of an adsorbed film through the process of adsorption of the polymer molecules on the metal surface.

4. Conclusions

Poly(vinyl alcohol-cysteine) acted as a good inhibitor for the corrosion of mild steel in 1 M HCl. Potentiodynamic curves revealed the mixed mode of inhibition of PVAC. Results obtained from different methods are in good agreement. The inhibition efficiency increases with an increase in concentration and immersion time. The activation energy of corrosion process of the inhibited solution was greater than the uninhibited solution. The enthalpy of activation reflects the endothermic metal dissolution and the entropy of activation reflects the decrease in rate of metal dissolution. The adsorption of PVAC follows the El-Awady isotherm. The thermodynamic parameters of adsorption suggest the spontaneity and physical nature of the process. The SEM images of mild steel reveal the formation of adsorbed film of PVAC.

Acknowledgements

One of the authors (AA) is grateful to the CSIR for the fellowship under Research Fellowship in Chemical Sciences for the Meritorious Students. The authors are thankful to the authorities of Avinashilingam University for Women for the encouragement.

References

- Abdel-Rehim, S.S., Khaled, K.F., Abd-Elshafi, N.S., 2006. Electrochemical frequency modulation as a new technique for monitoring corrosion inhibition of iron in acid media by new thiourea derivative. *Electrochim. Acta.* 51, 3269–3277.
- Ali Fathima Sabirneeza, A., Subhashini, S., Rajalakshmi, R., 2011. Water soluble conducting polymer composite of polyvinyl alcohol and leucine: an effective acid corrosion inhibitor for mild steel. *Mater. Corros.* 62, 9999.
- Ali Fathima Sabirneeza, A., Subhashini, S., 2012. A novel water soluble, conducting polymer composite mild steel acid corrosion inhibition. *J. Appl. Polym. Sci.*. <http://dx.doi.org/10.1002/APP.37661>.
- Ali, K.I., Wahdan, M.H., Hussein, M.A., 2009. New polymer syntheses, Part 43: novel polyamides-based diarylidene cyclopentanone: synthesis, characterization, and corrosion inhibition behavior. *J. Appl. Polym. Sci.* 112, 513–523.

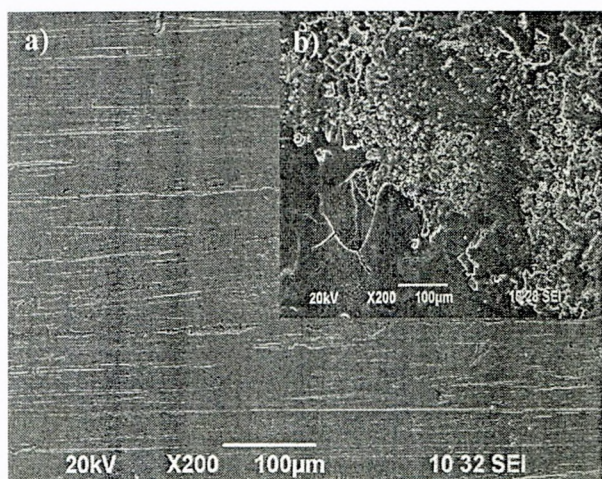


Figure 11 Scanning electron micrographs of mild steel (a) before immersion and (b) after immersion in 1 M HCl (6 h).

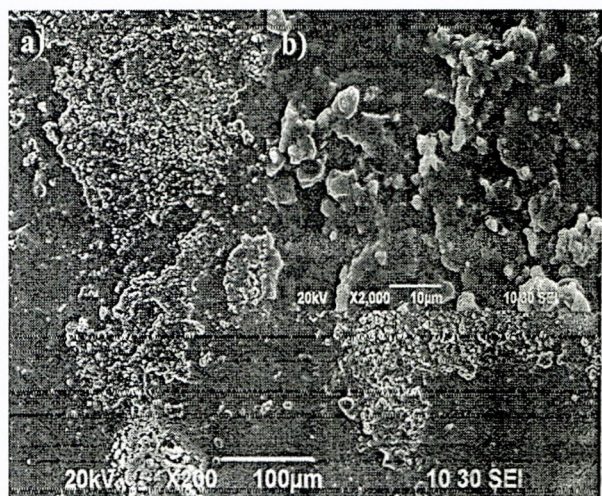


Figure 12 Scanning electron micrographs of mild steel after immersion in 0.6% PVAC + 1 M HCl (6 h) (a) X200 and (b) X2000.

- Amin, M.A., Abd El-Rehim, S.S., El-Sherbini, E.E.F., Hazzazi, O.A., Abbas, M.N., 2009. Polyacrylic acid as a corrosion inhibitor for aluminium in weakly alkaline solutions. Part I: weight loss, polarization, impedance EFM and EDX studies. *Corros. Sci.* 51, 658–667.
- ASTM G 1–2, Wear and Erosion; Metal Corrosion. 1996. Annual Book of ASTM Standards. ASTM, West Conshohocken, PA. 03.02, 89.
- Ayers, R.C., Hackerman, N., 1963. Corrosion inhibition in HCl using methyl pyridines. *J. Electrochem. Soc.* 110, 507–513.
- Benali, O., Larabi, L., Tabti, B., Harek, Y., 2005. Influence of 1-methyl 2-mercapto imidazole on corrosion inhibition of carbon steel in 0.5M H₂SO₄. *Anti-Corros. Method Mater.* 52, 280–285.
- Bentiss, F., Lebrini, M., Lagrenee, M., 2005. Thermodynamic characterization of metal dissolution and inhibitor adsorption processes in mild steel/ 2,5-bis(n-thienyl)-1,3,4-thiadiazoles/ hydrochloric acid system. *Corros. Sci.* 47, 2915–2931.
- Bentiss, F., Traisnel, M., Chaibi, N., Mernari, B., Vezin, H., Lagrenee, M., 2002. 2,5-Bis (n-methoxyphenyl)-1,3,4-oxadiazoles used as corrosion inhibitors in acidic media: correlation between inhibition efficiency and chemical structure. *Corros. Sci.* 44, 2271–2289.
- Breslin, C.B., Carrol, W.M., 1993. The activation of aluminium by indium ions in chloride, bromide and iodide solutions. *Corros. Sci.* 34, 327–341.
- Ebenso, E.E., Obot, I.B., 2010. Inhibitive properties, thermodynamic characterization and quantum chemical studies of secnidazole on mild steel corrosion in acidic medium. *Int. J. Electrochem. Sci.* 5, 2012–2035.
- Gelling, V.J., Wiest, M.M., Tallman, D.E., Bierwagen, G.P., Wallace, G.G., 2001. Electroactive-conducting polymers for corrosion control: 4. Studies of poly(3-octyl pyrrole) and poly(3-octadecyl pyrrole) on aluminum 2024–T3 alloy. *Prog. Org. Coat.* 43, 149–157.
- Gomma, M.K., Wahdan, M.H., 1995. Schiff bases as corrosion inhibitors for aluminium in hydrochloric acid solution. *Mater. Chem. Phys.* 39, 209–213.
- Granese, S.L., 1988. Study of the inhibitory action of nitrogen-containing compounds. *Corrosion* 44, 322–329.
- Granese, S.L., Rosales, B.M., Oviedo, C., Zebrino, J.O., 1992. The inhibition action of heterocyclic nitrogen organic compounds on Fe and steel in HCl media. *Corros. Sci.* 33, 1439–1453.
- Jayalakshmi, M., Muralidharan, V.S., 1998. Correlation between structure and inhibition of organic-compounds for acid corrosion of transition-metals. *Ind. J. Chem. Tech.* 5, 16–28.
- Jeyaprabha, C., Sathiyarayanan, S., Phani, K.L.N., Venkatachari, G., 2005a. Influence of poly(aminoquinone) on corrosion inhibition of iron in acid media. *Appl. Surf. Sci.* 252, 966–975.
- Jeyaprabha, C., Sathiyarayanan, S., Phani, K.L.N., Venkatachari, G., 2005b. Investigation of the inhibitive effect of poly(diphenylamine) on corrosion of iron in 0.5 M H₂SO₄ solutions. *J. Electroanal. Chem.* 585, 250–255.
- Khedr, M.G.A., Lashien, M.S., 1992. The role of metal cations in the corrosion and corrosion inhibition of aluminium in aqueous solutions. *Corros. Sci.* 33, 137–151.
- Labrabi, L., Harek, Y., Benali, O., Ghalem, S., 2005. Hydrazide derivatives as corrosion inhibitors for mild steel in 1 M HCl. *Prog. Org. Coatings* 54, 256–262.
- Lagrenee, M., Mernari, B., Bouanis, M., Traisnel, M., Bentiss, F., 2002. Study of the mechanism and inhibiting efficiency of 3,5-bis(4-methylthiophenyl)-4H-1,2,4-triazole on mild steel corrosion in acidic media. *Corros. Sci.* 44, 573–588.
- Musa, A.Y., Khadum, A.A.H., Mohamad, A.B., Daud, A.R., Takriff, M.S., Kamarudin, S.K., 2009. A comparative study of the corrosion inhibition of mild steel in sulphuric acid by 4,4-dimethylloxazolidine-2-thione. *Corros. Sci.* 51, 2393–2399.
- Negm, N.A., Salem, M.A.I., Zaki, M.F., 2009. Solubilization behaviors of non polar substrates using double tailed cationic surfactants. *J. Dis. Sci. Tech.* 30, 1167–1174.
- Negm, N.A., Zaki, M.F., 2008. Corrosion inhibition efficiency of nonionic schiff base amphiphiles of p-amino benzoic acid for aluminium in 4N HCl. *Colloid Surf. A: Physiochem. Eng. Aspec.* 322, 97–102.
- Obot, I.B., Obi-Egbedi, N.O., Umoren, S.A., 2009. Adsorption characteristics and corrosion inhibitive properties of clotrimazole for aluminium corrosion in hydrochloric acid. *Int. J. Electrochem. Sci.* 4, 863–877.
- Oguzie, E.E., 2006. Studies on the inhibitive effect of occimum viridis extract on the acid corrosion of mild steel. *Mater. Chem. Phys.* 99, 441–446.
- Quraishi, M.A., Khan, S., 2005. Thiodiazoles-A potential class of heterocyclic inhibitors for prevention of mild steel corrosion in hydrochloric acid solution. *Ind. J. Chem. Tech.* 12, 576–581.
- Quraishi, M.A., Sardar, R., 2003. Hector bases – a new class of heterocyclic corrosion inhibitors for mild steel in acid solutions. *J. Appl. Electrochem.* 33, 1163–1168.
- Shukla, S.K., Quraishi, M.A., Prakash, R., 2008. A self doped conducting polymer “polyanthranilic acid”: an efficient corrosion inhibitor for mild steel in acidic solution. *Corros. Sci.* 50, 2867–2872.
- Shukla, S.K., Ebenso, E.E., 2011. Corrosion inhibition, adsorption behavior and thermodynamic properties of streptomycin on mild steel in hydrochloric acid medium. *Int. J. Electrochem. Sci.* 6, 3277–3291.
- Singh, A.K., Quraishi, M.A., 2011. Investigation of the effect of disulfiram on corrosion of mild steel in hydrochloric acid solution. *Corros. Sci.* 53, 1288–1297.
- Srikanth, A.P., Sunitha, T.G., Nanjundan, S., Rajendran, N., 2006. Synthesis, characterization, and corrosion protection properties of poly (N-(acryloyloxymethyl) benzotriazole-co-methyl methacrylate) on mild steel. *Prog. Org. Coat.* 56, 120–125.
- Taha, A.A., Selim, I.Z., Khedr, A.A., 1995. Evaluation of some amino acids as corrosion inhibitor for steel in sulphuric solutions at different temperatures. *Egypt. J. Chem.* 38, 141–149.
- Umoren, S.A., 2009. Polymers as corrosion inhibitors for metals in different media-A review. *Open Corros. J.* 2, 175–188.
- Umoren, S.A., Ebenso, E.E., Okafor, P.C., Ogbobe, O., 2006. Water-soluble polymers as corrosion inhibitors. *Pigm. Resin. Technol.* 35, 346–352.
- Wahyuningrum, D., Achmad, S., Syah, Y.M., Buchari, B., Bundjali, B., Ariwahjoedi, B., 2008. The correlation between structure and corrosion inhibition activity of 4,5-diphenyl-1-vinylimidazole derivative compounds towards mild steel in 1% NaCl solution. *Int. J. Electrochem. Sci.* 3, 154–166.
- Yurt, A., Balaban, A., Ustün Kandemir, S., Bereket, G., Erk, B., 2004. Investigation on some schiff bases as HCl corrosion inhibitors for carbon steel. *Mater. Chem. Phys.* 85, 420–426.
- Yurt, A., Bereket, G., Ogretir, C., 2005. Quantum chemical studies on inhibition effect of amino acids and hydroxy carboxylic acids on pitting corrosion of aluminium alloy 7075 in NaCl solution. *J. Mol. Struct. Theochem.* 725, 215–221.
- Yurt, A., Buetuen, V., Duran, B., 2007. Effect of the molecular weight and structure of some novel water-soluble triblock copolymers on the electrochemical behaviour of mild steel. *Mater. Chem. Phys.* 105, 114–121.